From Hit to Lead. Analyzing Structure−Profile Relationships

Rébecca Poulain,*,† Dragos Horvath,†,‡ Béatrice Bonnet,†,⊥ Christian Eckhoff,§ Béatrice Chapelain,|| Marie-Christine Bodinier,§ and Benoît Déprez†,⊥

Department of Chemistry, CEREP, 1 rue du Pr. Calmette, F-59000 Lille, France, Department of Pharmaceutical Development, CEREP Inc., 15318 NE 95th Street, Redmond, Washington 98052, and Department of Pharmacology, CEREP, Celle l'Evescault, BP1, F-86600 Le Bois L'Evêque, France

Received March 14, 2001

Two compounds, obtained by random screening, and displaying micromolar activities on the μ opiate receptor were used as starting points for optimization. In that work, the traditional concept of the activity of a compound (related to one or a few targets) was extended to the comprehensive pharmacological profile of that compound on more than 70 receptors, transporters, and channels relevant to a CNS-oriented project. Using the two complementary design strategies based on two similarity concepts described in the previous paper, we have obtained analogues with IC_{50} values ranging between 0.9 nM and a few micromolar on the μ receptor and displaying qualitatively different profiles. We discuss here, both on a case-by-case basis and from a statistical standpoint, the pharmacological profiles in light of the two similarity concepts.

Introduction

The acceleration of the primary steps of drug discovery has recently shifted the bottlenecks toward the selection[1] of compounds, among numerous primary hits, that will be optimized to obtain eventually a potent, nontoxic, and orally available drug. Until recently, most of the optimization effort was directed toward the potency of the leads against the target of interest, and selectivity among subtypes, whereas the equally important aspects of specificity and bioavailability were, most of the time, addressed at the end of a potency optimization cycle, sometimes disqualifying the obtained candidates.

Early monitoring of the specificity and bioavailability during hit-to-lead optimization might be used to drive the design process and to avoid potential dead ends during the drug development. However, a systematic assessment of all the constraints that have to be obeyed by a drug candidate at all the stages of the optimization process would be a practically unfeasible task.

In this work we explore the use, in hit optimization, of "pharmacological profiling"—an array of in vitro binding experiments against a set of relevant biological targets which in our opinion represent a reasonable tradeoff between the implied experimental effort and the acquired pharmacological information. The pharmacological profile of a compound, obtained from robotized high-throughput profiling (HTP) experiments, is a table of binding data against a panel of receptors, channels, and transporters.

The pharmacological profile can be therefore viewed as a generalization of the classical concept of activity (e.g., the scalar value of activity on a given target), representing an "activity vector" in the "space of pharmacological profiles". In this context, the classical structure−activity relationships (SARs), which represent the basis of medicinal chemistry and drug design, have been generalized and adapted to the novel vectorial definition of biological activity, and are referred to here as structure−profile relationships.

The purpose of this study was to evidence how chemical structures relate to their activity profiles, to define the first steps of an optimal "design and selection" process for lead identification.

In this work, we have pursued our proof-of-concept on the μ opiate receptor.[2] Until now, most studies on opiate ligands have focused on selectivity among the three receptor types (μ, δ, κ)[3] rather than specificity against more distantly related G-protein-coupled receptors (GPCRs).[4] Out of the primary hits, obtained by random screening on the μ(rat) receptor, compounds **1** and **2** (Chart 1) were selected as starting points for an optimization cycle. They are similarly active on the opiate receptors but however exhibit rather different pharmacological profiles. Indeed, compound **1** showed a high specificity toward the opiate receptors, and therefore represented an obvious choice for optimization. By contrast, compound **2**, of affinity similar to that of **1**, had a poor specificity and was selected as an alternative starting point for optimization.

Overall, several hundreds of analogues were designed, synthesized, and screened. They included, on one hand, compounds retrieved by pharmacophore-pattern-oriented similarity searching against a virtual library of potentially synthesizable combinatorial products and, on the other hand, exploratory analogues, some of which introduced drastic changes of the pharmacophoric patterns of their parent compounds. Pharmacological profiles of 45 selected analogues were then determined.

* To whom correspondence should be addressed. Current address: UMR8525, Faculté des Sciences Pharmaceutiques et Biologiques, Chimie Organique, 3 rue du Pr. Laguesse, BP 83, F-59006 Lille Cedex, France. Phone: 33.3.20.96.47.07. Fax: 33.3.20.96.47.09. E-mail: rpoulain@phare.univ-lille2.fr.

† Department of Chemistry.

‡ Current address: CEREP, 128 rue Danton, BP50601, F-92506 Rueil-Malmaison, France.

§ Department of Pharmaceutical Development.

|| Department of Pharmacology.

⊥ Current address: Devgen NV, Technologiepark 9, B-9052 Ghent, Zwijnaarde, Belgium.

10.1021/jm010878g CCC: $20.00
Published on Web 09/11/2001

Chart 1

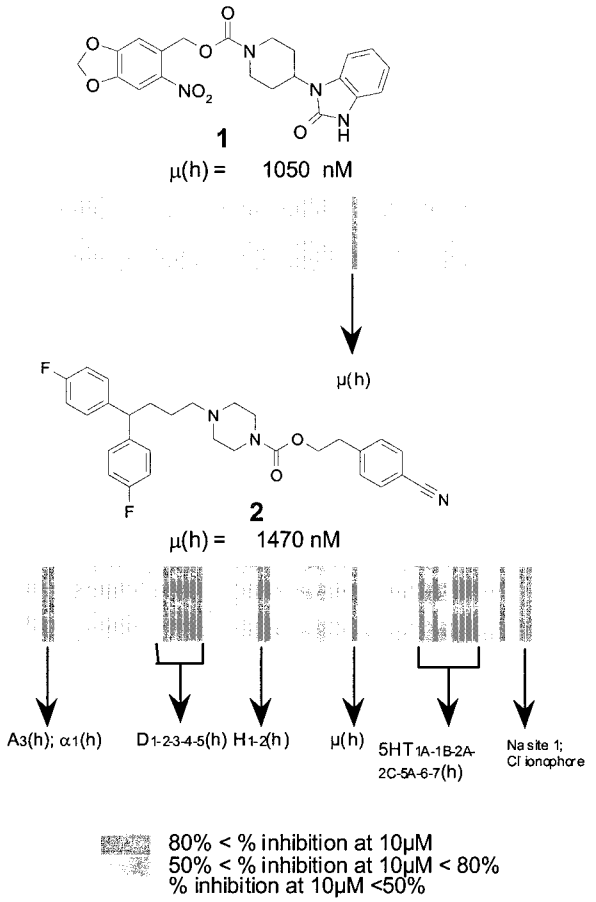

In this paper we report the structure−profile relationships of these analogues. Both a detailed case-by-case analysis of the pharmacological profiles and a statistical study, using similarity−dissimilarity metrics, were performed and are discussed.

Chemistry

To investigate in a systematic way the structural space around **1** and **2**, two independent methods of analogue design have been used for both hits. Method A consists of varying the distribution of the *pharmacophoric*[5] elements of the active compound while keeping a similar molecular topology. In contrast, method B[6] aims at retrieving analogues that possess a similar pharmacophoric pattern, out of a virtual library of all feasible combinations of available starting materials (more than 7000 diversity reagents, in our case). This method relies on (1) algorithms for rapid generation of 3D molecular fingerprints[7] (FBPAs) based on multiconformational models and (2) similarity[8] evaluation tools relying on these 3D fingerprints for the design of analogues (FBPA dissimilarity score).

The 35 selected analogues of **1** are presented in Charts 2−4.[9] They are subdivided into three series. The first series (analogues **3**−**16**) consists of analogues in which a topology similar to that of **1** was conserved while changes in substituents, linkers, and cycles were introduced (method A). The second series (analogues **17**−**31**) was retrieved by similarity searching using FBPAs (method B). The last series (analogues **32**−**37**) consists of "hybrid" compounds displaying key features evidenced by each analoging method.

Chart 2

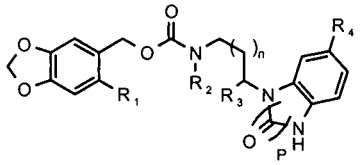

	R_1	R_2	R_3	R_4	n	p
1	NO_2	$-CH_2-CH_2-$		H	1	1
3	Cl	$-CH_2-CH_2-$		H	1	1
4	Cl	H	H	H	1	1
5	Cl	H	H	H	0	1
6	Cl	$-CH_2-CH_2-$		H	1	2
7	Cl	$-CH_2-CH_2-$		CH_3	1	1

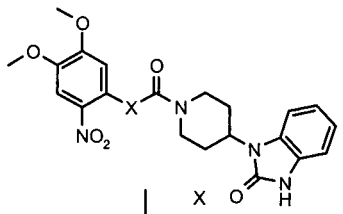

	X
8	CH_2
9	-CH=CH-

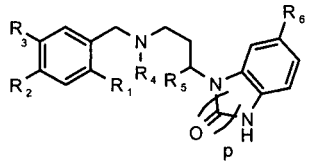

	R_1	R_2	R_3	R_4	R_5	R_6	p
10	Cl	$-OCH_2O-$		$-CH_2-CH_2-$		H	1
11	Cl	$-OCH_2O-$		H	H	H	1
12	NO_2	$-OCH_2O-$		$-CH_2-CH_2-$		H	1
13	NO_2	$-OCH_2O-$		$-CH_2-CH=$		H	1
14	Cl	$-OCH_2O-$		$-CH_2-CH_2-$		H	2
15	Cl	$-OCH_2O-$		$-CH_2-CH_2-$		CH_3	1
16	Cl	CH_3	H	$-CH_2-CH_2-$		H	1

The same analogue design strategies allowed to analogues of **2** to be obtained. In particular, the analogues of **2** generated by method A (similar topology) explore (1) shortening of the chain between the benzhydryl moiety and the basic nitrogen, (2) variation of the substituents of the aromatic rings, (3) changing the piperazine ring for 4-aminopiperidine (producing analogues with modified shape and pK_a), and (4) suppression of one of the aromatic rings of the benzhydryl group. These transformations required the synthesis of special precursors such as amine **38** (Scheme 1). A selection of amines was reacted with different phenethyl derivatives (Scheme 2) to give 131 different analogues of **2**. Table 1 summarizes the analogues **39**−**46** selected for further evaluation.

Among the analogues found by a similar pharmacophoric pattern search (method B), many compounds shared either the 4-cyanophenethyl group or the benzhydryl moiety with **2**. Nevertheless, other analogues presented a completely different topology (compounds **47** and **48**, Chart 5), while still featuring two aromatic rings, a positive charge, and a fairly flexible carbon chain.

Chart 3

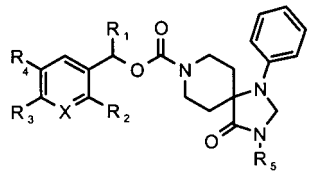

	R_1	R_2	R_3	R_4	R_5	X
17	H	NO_2	-OCH_2O-		H	CH
18	H	Cl	-OCH_2O-		$CH_2CONHCH_3$	CH
19	H	Cl	-OCH_2O-		H	CH
20	H	H	-OCH_2O-		H	CH
21	H	H	thiadiazole		H	CH
22	H	H	H	-OC_6H_5	H	CH
23	-CH_2-CH_2-		H	H	H	CH
24	H	H	H	H	H	N

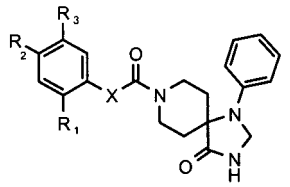

	R_1	R_2	R_3	X
25	H	-OCH_2O-		-CH_2NH-
26	NO_2	-OCH_2O-		-CH=CH-
27	NO_2	OCH_3	OCH_3	-CH=CH-

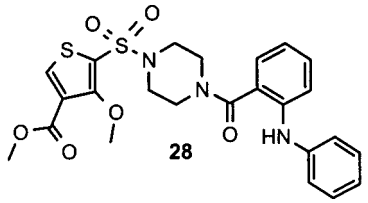

28

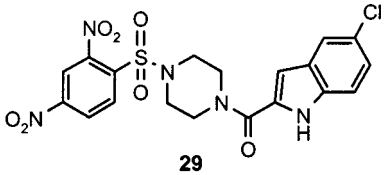

29

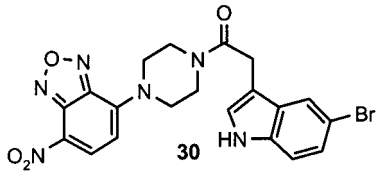

30

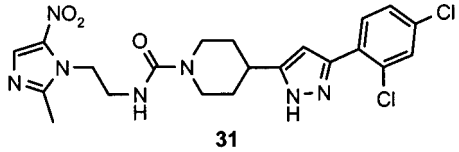

31

Eventually, 35 analogues of **1** and 10 analogues of **2** were submitted to HTP experiments.

HTP Experiments

The pharmacological profile of a compound, obtained from robotized experiments, is expressed as the series

Chart 4

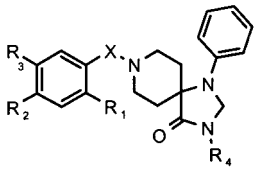

	R_1	R_2	R_3	X	R_4
32	Cl	-OCH_2O-		-CH_2-	H
33	Cl	-OCH_2O-		-CH_2-	$CH_2CONHCH_3$
34	H	-OCH_2O-		-CH_2-	H
35	H	thiadiazole		-CH_2-	H
36	H	H	-OC_6H_5	-CH_2-	H
37	Cl	-OCH_2O-		-CH_2OCO-	CH_2COOH

Scheme 1[a]

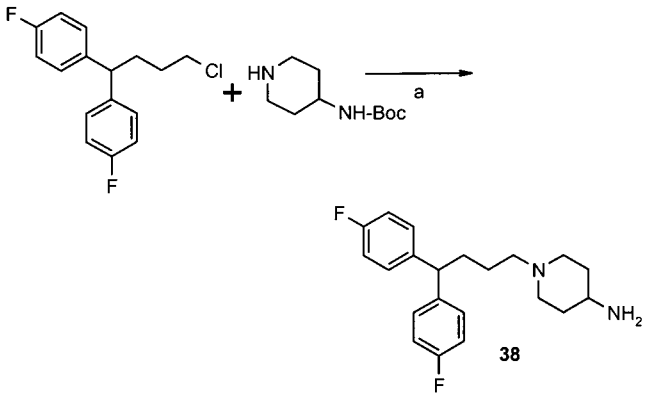

[a] Reagents and conditions: (a) (i) CH_3CN, DIPEA, reflux, 4 days; (ii) HCl (3 N), EtOH, reflux, 2 h.

of percentages of radioligand displacement by a 10 μM solution of compound in a panel of binding tests involving receptors, channels, and transporters (Table 2). The choice of the biological receptors was done considering, in a CNS project, the balance between the experimental effort and the acquired pharmacological information, and included a large proportion of biogenic amines and peptide GPCRs.

All compounds were primarily tested on all receptors at a single concentration, allowing a fast discrimination between "active" and "inactive" compounds.[10] Indeed, in given testing conditions, pIC_{50} values behave, though not linearly, at least monotonically as a function of the percentage of inhibition. In particular, tested at 10 μM, a compound displacing more than 80% of the radioligand is likely to have an IC_{50} below 2 μM, which is a realistic threshold used by most screeners to define a hit.[11]

In a second step, dose−response curves were generated and IC_{50} values calculated for all compounds displaying a percentage of inhibition superior to 80% at 10 μM. Two hundred IC_{50} values were calculated, among the 3240 (75 receptors × 45 analogues) receptor−compound interactions previously evaluated (Table 3).

Results and Discussion

Two main categories of targets were evidenced at this testing concentration for our chemical series. On one

Scheme 2[a]

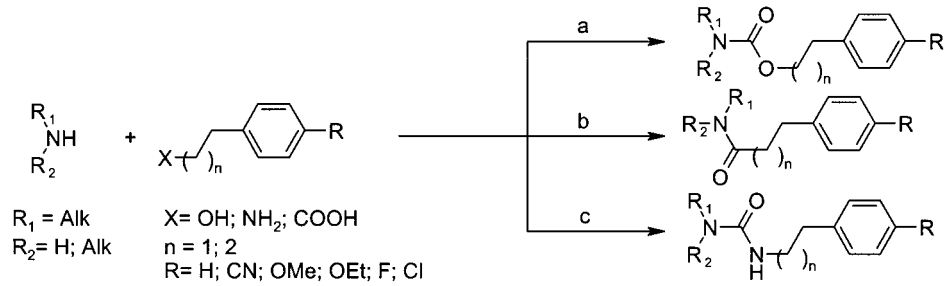

[a] Reagents and conditions: (a) (i) alcohol in DMF, *N*,*N*′-carbonyldiimidazole (CDI) in THF; (ii) amine in DMF, 88−96%; (b) (i) carboxylic acid in DMF, CDI in THF; (ii) amine in DMF, 90−92%; (c) (i) amine in DMF, CDI in THF; (ii) amine in DMF, 85−91%.

Table 1. Analogues of **2** Retrieved by Method A (Similar Topology)

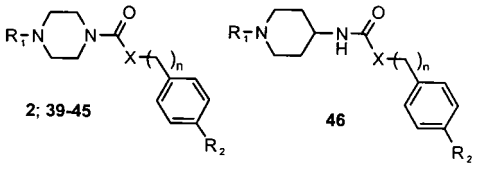

compd no.	R_1	*n*	X	R_2
2	4,4-bis(4-fluorophenyl)butyl	2	O	CN
39	4,4-bis(4-fluorophenyl)butyl	2	O	F
40	4,4-bis(4-fluorophenyl)butyl	1	CH_2	F
41	3-phenylpropyl	2	O	CN
42	3-phenylprop-2-enyl	2	O	CN
43	3-phenylpropyl	2	O	OC_2H_5
44	4,4-bis(4-fluorophenyl)butyl	2	NH	OC_2H_5
45	4,4-bis(4-fluorophenyl)butyl	2	CH_2	H
46	4,4-bis(4-fluorophenyl)butyl	2	O	CN

Chart 5

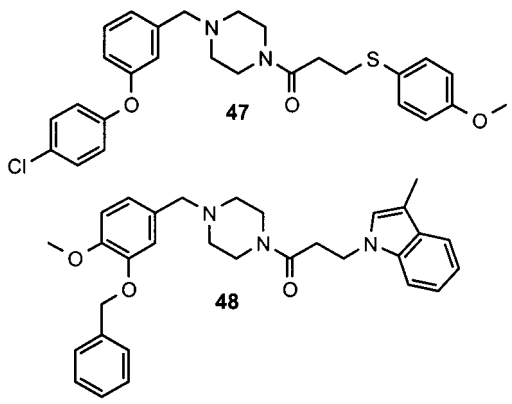

hand, receptors that bind to low molecular weight endogenous monoamines (some G-protein-coupled receptors and monoamine transporters) and cation channels showed a "high hit rate" in our series. On the other hand, receptors of rather large peptides (galanine, VIP) or small uncharged ligands (CB_1, CB_2) displayed lower hit rates for our series. Out of the 72 receptors (apart from the opiate receptors), only 35 happened to interact with our compounds at the level defined above.

(a) Structure−Profile Relationships of Analogues of 1. Introduction of a Basic Nitrogen Has a Dramatic Effect on the Pharmacological Profile. Expectedly, the apparition of a positive charge at the piperidine moiety leads to a general increase of activity on the opiate receptors. However, it also introduces secondary activities in the profile (Table 3). Compounds **10**−**16** are in general less specific than the corresponding carbamates and amides where the piperidine has lost its basic character. This observation is confirmed by the comparison of compounds **17**−**24** (uncharged) with compounds **32**−**36** (positively charged), where the benzimidazolone moiety is replaced by a phenyltriazaspirodecanone. Most susceptible to that change are the muscarinic acetylcholine receptors and the dopamine receptors.

Substitution at the *ortho*-Position of the Benzyl Moiety Enhances the Specificity of the Compounds. Analogue **10** that bears an *o*-nitro group at the benzyl moiety is more specific than compounds **16** and **34**−**36**. Interestingly, substitution by a chlorine atom at that position is less beneficial. Indeed, *o*-chloro compounds (**3**, **10**, and **19**) are consistently less specific that their *o*-nitro counterparts (respectively **1**, **12**, and **17**). Noteworthy, the replacement of the chlorine atom by a nitro group totally abolished the activity on ORL-1 while keeping binding to opiate receptors unchanged. Moreover, in our series, this position is the only one where SARs for opiate receptors and ORL-1 diverge.

Benzothiadiazole Is a Good Bioisosteric Replacement of the Methylenedioxyphenyl Group. In a similarity study based on the Kohonen neural network, Anzali et al. showed previously that the electronic distribution of these groups are almost equivalent.[12] In our FBPA-based similarity metric the two moieties appear also to be very close together. Experimentally, in our hands, the replacement of the methylenedioxy (**20** and **34**) by a thiadiazole (respectively **21** and **35**) led in the two instances to almost identical pharmacological profiles, generalizing the observation of Anzali et al. on the ET_A receptor.[12]

1-Phenyl-1,3,8-triazaspiro[4.5]decan-4-one and 1-Piperidin-4-yl-1,3-dihydrobenzimidazol-2-one Are Not Universally Interchangeable. Despite obvious differences in their molecular backbones, these two moieties have very similar FPBAs. Moreover, the two moieties seem to be equivalent for the opiate receptors and ORL-1.[13] However, the profile of their respective compounds differs (compare the profiles of **10** and **32**). More intriguingly, relatively subtle modifications of the benzimidazolone moiety, such as the imidazolidine ring expansion to form a quinoxaline (**6** and **14**) or the introduction of a methyl group at the 6 position (**7** and **15**), led to drastic changes in the profile, and in general to an improvement of the selectivity for opiate receptors (compare **6** and **7** to **3** as well as **14** and **15** to **10**). Interestingly, the substitution of the hydrogen at N-3

Table 2. Biological Targets for the Binding Tests in HTP

receptor	subtype[a,b]	receptor	subtype[a,b]
adenosine	A_1 (h)	muscarinic	M_1 (h)
	A_{2a} (h)		M_2 (h)
	A_3 (h)		M_3 (h)
adrenergic	(ns) α_1		M_4 (h)
	(ns) α_2		M_5 (h)
	β_1 (h)	neurokinin	NK_1 (h)
	β_2 (h)		NK_2 (h)
	NE uptake (h)		NK_3 (h)
angiotensin-II	AT_1 (h)	neuropeptide Y	Y_1 (h)
	AT_2 (h)		Y_2 (h)
atrial natriuretic peptide	(ns) ANP	neurotensin	NT (h)
		opiate	μ (h)
benzodiazepine	central BZD		δ (h)
	peripheral BZD		κ (h)
bombesin	(ns)	orphanin	ORL1 (h)
bradykinin	B_2 (h)	PACAP	null (h)
calcitonin gene-related peptide	(ns) CGRP (h)	phencyclidine	PCP
		prostanoid	TXA_2/PGH_2 (h)
cannabinoïds	CB_1 (h)		PGI_2 (h)
	CB_2 (h)	purinergic	P_{2X}
chemokine	CCR1 (h)		P_{2Y}
cholecystokinin	CCK_A (h)	serotonin	5-HT_{1A} (h)
	CCK_B (h)		5-HT_{1B}
dopamine	D_1 (h)		5-HT_{2A} (h)
	D_2 (h)		5-HT_{2C} (h)
	D_3 (h)		5-HT_3 (h)
	$D_{4,4}$ (h)		5-HT_{5A} (h)
	D_5 (h)		5-HT_6 (h)
	DA uptake (h)		5-HT_7 (h)
endothelin	ET_A (h)	sigma	(ns) σ
	ET_B (h)	somatostatin	(ns)
GABA	(ns)	vasoactive intestinal peptide	(ns) VIP
galanin	GAL-1 (h)		
growth factors and cytokines	PDGF		
	IL-8A (h)	vasopressin	V_{1A} (h)
	TNF-α (h)	Ca^{2+} channel	L verapamil site
histamine	central H_1	K^+ channel	voltage-dependent
	H_2		Ca^{2+}-dependent
melatonin	ML_1	Na^+ channel	site 2
		Cl ionophore	TBPS site

[a] ns is for nonselective. [b] h is for human.

of the triazaspirodecanone by a *N*-methylacetamide gave compounds both more active on the opiate receptors and more specific (compare **19** and **32** to their substituted analogues **18** and **37**, respectively). Moreover, the corresponding acetic acid derivative, though far less active on the opiate receptors, exhibits no detectable binding to the other receptors of our profile. We show with these two specific examples the interest of the similarity-based analogue design. Indeed the replacement of the benzimidazolone by the spirocyclic moiety, proposed by method B, allowed the identification of compounds that fulfill the pharmacophore requirements of the opiate receptor while offering a position where various substitutions can be made without affecting the target activity. The chemist is therefore in a very favorable situation to improve both the specificity and the physical−chemical properties of the compound.

(b) Structure−Profile Relationships of Analogues of 2. Compounds Containing a Benzhydryl Moiety are Promiscuous. Compound **2** and its benzhydryl analogues **39**, **40**, **44**, and **46** are rather weak opiate ligands, and exhibit dopaminergic and serotoninergic profiles. Both **44** and **39** bind to the sodium channel with IC_{50} values of 165 and 1800 nM, respectively. Compound **46**, where the piperazine is replaced by a 4-aminopiperidine, is the most promiscuous compound in that experiment. This may be due to a greater flexibility. On the contrary, the removal of one aromatic ring from the benzhydryl side led to a great improvement of both specificity and binding to the opiate receptors (**41**−**43**). Combined removal of one aromatic ring of the benzhydryl moiety and shortening of the alkyl chain enhanced specificity for μ, providing the best compound in this series (**42**) with an IC_{50} of 197 nM on μ.[14] Interestingly, selectivity among opiate receptors was also achieved. Comparison of **41** and **43** showed that a residual activity on H_1 can be linked to the presence of a nitrile function.

Four structurally related compounds (Chart 6), the vasodilatator flunarizine (Na^+ channel ligand with an IC_{50} of 340 nM[15]), the antipsychotic pimozide (dopamine antagonist), and GBR13069 and GBR12909 (dopamine transporter ligands), were submitted to binding assays on opiate receptors (Table 4) to compare them with molecule **2** and its analogues. These four compounds, sharing a benzhydryl moiety with **2**, all show, like **2** and its analogues, micromolar or submicromolar binding affinities for μ besides their target activities. Conversely **2** and its analogues bind to the primary targets of these four compounds.

Compounds can thus be sorted into three categories of rather homogeneous behaviors: (1) analogues of **1** devoid of basic nitrogen, which are rather specific of opiate receptors though displaying only micromolar

Table 3

	IC$_{50}$(nM)[a,b]																																					
Nº	μ	κ	δ	ORL$_1$	A$_1$	A$_3$	α_1 (ns)	β_1	NE uptake	Peripheral BZD	CB$_1$	D$_1$	D$_2$	D$_3$	D$_{4.4}$	D$_5$	DA uptake	H$_1$ (central)	H$_2$	M$_1$	M$_2$	M$_5$	ML$_1$	NK$_1$	NK$_2$	5-HT$_{1A}$	5-HT$_{1B}$	5-HT$_{2A}$	5-HT$_{2C}$	5-HT$_3$	5-HT$_{5A}$	5-HT$_6$	5-HT$_7$	σ (ns)	V$_{1a}$	L-type verapamil Ca^{2+} channel	Na$^+$ channel (site 2)	Cl$^-$ ionophore
1	1050																																					
3	147	284	2530		2640	1780	1340		3020	1040		7580				4890							1740		4420	4650	708								2220			2380
4	2480	1740			344	3330																																
5																																						
6	2590	1060																																				
7	1235	797	5640																																			
8		1320																																				
9	960	4030					2010																															
10	1.2	1.7	37.4	38			1330							1910						630	518	1910											762					
11	235	507	3330				174					2500			429																			328				
12	1.5	37	264																																			
13	19.3	311	1040																											4420								
14	6.3	32	620	434											6550		1520																					
15	2.4	2.9	117	283			4920													556													663			1710		
16	16	270	1410	1910			1150					2740	480	154	1690					1780	1570												849			1340		
17		5070																																				
18	179	333	1765													3660																						
37	735	6570																																				
19	1730	2145				5470																							1830						6650			
20	2285	2235																																	2010			
21		1480																																				
22		1810				1510											2940									2080			652									
23	1470	617												3180															345						5160			
24		3550																																				
25		2280																																				
26																																						
27																																						
28	4955	7240																																				
29	2285																																					
30		1010																																				
31	2890		7130																																			
32	2.0	5.7	138	97										2120																				581		1110		
33	0.9	2.1	11.4	19									2120	1930																								
34	16.7	56.1	1190	340									557	160	947																							
35	24.9	104	4120	758			4250						123	29	1880																							
36	83.5	101	1840	2420			2830	3590	2810				538	149			2250		496		4540													1250		552		
2	1470					3480	1100					1120	2240	195	776	988	996	795	1030							1020		715			3380	2280	1440	702		1720	1350	3520
39	4015	4230				4210	1640						2620	456	338	1550	1650	1280	1250							1140		1060	3450			1530	726			2730	1800	
40	3660	2820	9380			5080	1170							977	716	3020	1280	1660	1340							1110		1030				1350	1170			4300	737	
41	800														1410			280								1570		854										
42	197																																					
43	1690					4180																						980					1430	2170				
44	4545	4120	8570			2460	993					967	2890	341		1450	994	1820	757					839	5180			231	1420			800	2040	482		860	438	
45	3810	2150	3710				2190					2750		758	280	1860	954	1930	1980									950	4070		5520	7780	2130			2350	539	
46	6545	1980	5770			5980	417		1140		6090	376	551	538	543	513	781	454	368							985	3580	683	2760			427	998		3650	284	165	
47		2200				3750																																
48	3950	3580				3730																														4840	1480	

[a] Binding affinities (IC$_{50}$) of reference compounds **1** and **2** and of their analogues **3**−**37** and **39**−**48**, respectively, on the targets on which inhibition at 10 μM exceeded 80%. [b] IC$_{50}$ values below 2 μM are white on a black background.

Chart 6

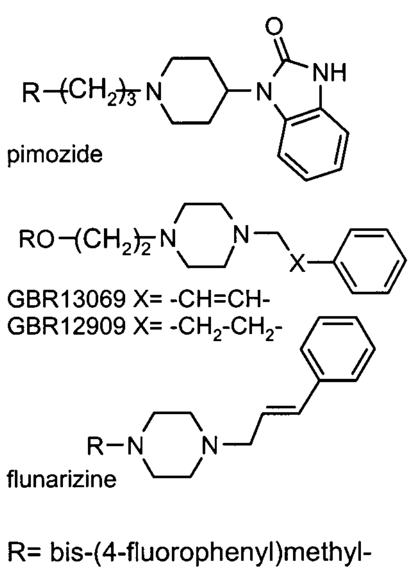

activities; (2) analogues of **1** with a basic nitrogen, which appear to be less specific, but still have a ratio of IC$_{50}$-(other target)/IC$_{50}$(opiate) of 30 or more; (3) analogues of **2**, which are poorly specific. The structural modifications undertaken during optimization have thus, as expected, a strong impact on the pharmacological profile of the compounds.

(c) Statistical Study. Structural Neighbors of Promiscuous Compounds Are in General Promiscuous. As a conceptual frame useful for the discussion of structure−profile relationships, the profile of each analogue can be viewed as a "point" of the vectorial activity space, whereas its structure is unambiguously positioned in a pharmacophore-pattern-based descriptor space (structure space) with a well-defined similarity metric.

For the statistical analysis, we have purposely chosen to work with percentages of inhibition at 10 μM and not with IC$_{50}$ or even pK_i. Indeed, these percentages can be readily obtained for a large number of compounds (here, 47 compounds) and targets (here, 75 including μ, κ, and δ). Moreover, they have been shown to behave monotonically as a function of IC$_{50}$. A first analysis of the correlation between pharmacological profile dissimilarity and pharmacophoric pattern dissimilarity is given in Figure 1, where all the compounds of this study are represented as disks of radius related to the number of receptors hit at 10 μM (for a threshold of 50% inhibition):

$$\text{radius} = (0.5N_{50-80} + N_{80-100})/75$$

Table 4. Binding Affinities (IC_{50}) on the Opiate Receptors of Some Reference Ligands

		IC_{50} (nM)[a,b]		
entry	name	μ (h)	κ (h)	δ (h)
1	pimozide	372 (26−719)	990 (707−1270)	3760 (3000−4520)
2	flunarizine dihydrochloride	2410 (2407−2420)	9480 (5020−14000)	3630 (3620−3640)
3	GBR13069·2HCl	2690 (2320−3060)	1770 (1730−1800)	>10000
4	GBR12909·2HCl	3530 (2790−4270)	2140 (2100−2180)	>10000

[a] IC_{50} values were obtained from an experiment performed in duplicate from 11 concentrations; both values are given in parentheses. [b] The radioligands used were [^{3}H]DAMGO (μ (h)), [^{3}H]U69593 (κ (h)), and [^{3}H]DPDPE (δ (h)).

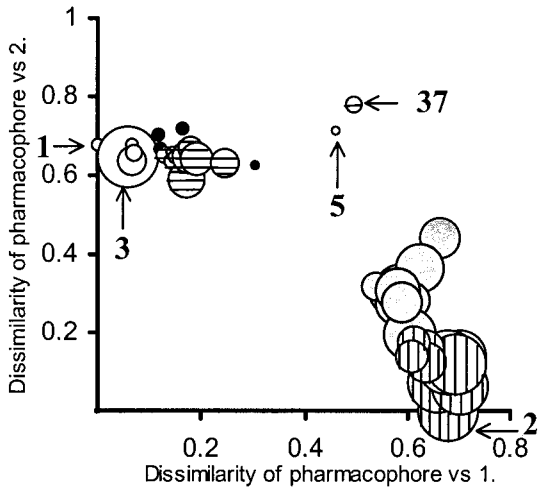

Figure 1. Radius of the disk as a function of the number of targets hit by the compound (calculated from percentages of inhibition at 10 μM): analogues of **2**, vertically striped; analogues **10**−**16** and **32**−**36** of **1**, gray; analogues **3**−**9** of **1**, white; analogues **17**−**27** of **1**, horizontally striped; analogues **28**−**31** of **1**, black.

where N_{a-b} is the number of receptors for which the percentage of inhibition at 10 μM by the compound was in the range $a-b$. This analysis thus does not take the nature of the biological target into consideration. It defines the promiscuity of a compound within a given set of targets.

The *X*-axis of Figure 1 represents the score of dissimilarity of pharmacophore (FBPA metric) between the compound of interest and **1**. In the same way, the *Y*-axis represents the score of dissimilarity of pharmacophore between the compound of interest and **2**. Necessarily, **1** is located on the *Y*-axis and **2** on the *X*-axis (see the pointing arrows in Figure 1).

All the analogues of compound **2**, independently of the analoging method used for their design, have a pharmacophoric pattern similar to that of **2** ($\Delta Y < 0.2$) and are quite dissimilar to **1** (*X* about 0.7). They are rather promiscuous for our test panel (large disks).

Analogues **3**−**9** of parent compound **1**, designed with similar topologies, have a pharmacophoric pattern similar to that of **1** ($\Delta X < 0.15$) and are quite dissimilar to **2** (*Y* about 0.7). As their parent **1**, these analogues, except the outlier **3**, do not hit many targets (small disks). Analogues **17**−**31** designed by a pharmacophore-oriented search are also represented as small disks. Interestingly, both the benzimidazolone (compounds **10**−**16**) and triazaspirodecanone (compounds **32**−**36**) series of analogues of **1** with a basic nitrogen are found by our pharmacophore similarity metric closer to **2** (*X* about 0.6, and $0.2 < Y < 0.5$). This is due to the presence of the basic nitrogen. Their total count of hit targets is also larger due to the favorable interactions of these compounds with many G-protein-coupled receptors.

The pharmacophorically quite dissimilar **37** and **5** show, like **1**, little affinity for most of the targets of the pharmacological profile. Surprisingly, **37**—carrying a carboxylate group (net negative charge)—maintains nevertheless a measurable activity on the μ receptor.

It is thus clear from Figure 1 that the clusters of compounds observed in the 2D space defined by the dissimilarity scores with respect to the two reference hits **1** and **2** coincide fairly well with the classification of the compounds in terms of their promiscuity on our panel of receptors: compounds with a pharmacophore similar to that of **1** are, like **1**, quite specific in our pharmacological profile, whereas compounds with a pharmacophore similar to that of **2** are, like **2**, more promiscuous for this profile.

Differences in Pharmacophoric Pattern Translate Well into Differences in Pharmacological Profile. An activity dissimilarity score "NR_{diff}(A,B)" of the pharmacological profiles of two compounds, A and B, is then defined as a fuzzy counter of the number of receptors within the profile with respect to which A and B behave "differently"

$$NR_{diff}(A,B) = \sum_{\text{tests } i} \Delta(|\%\ \text{inh}_i(A) - \%\ \text{inh}_i(B)|)$$

where % inh_i stand for the percentages of inhibition (at 10 μM) of A and B in the test *i* among the 75 tests of the profile.

$$\Delta(|\%\ \text{inh}_i(A) - \%\ \text{inh}_i(B)|)$$

is an empirical measure of how different the two compounds behave with respect to that test:

$$\Delta(x) = \begin{cases} 0 \text{ if } x \le 30 \\ (x - 30)/40 \text{ if } 30 < x \le 70 \\ 1 \text{ if } x > 70 \end{cases}$$

The above-defined NR_{diff} score can be regarded as a semiquantitative dissimilarity metric of the activity profiles of compounds. Obviously, two molecules both scoring 100% inhibition in the same test may nevertheless strongly differ in their actual binding affinity.

The choice of the target panel in profiling experiments is subject to many and often contradictory constraints. On one hand, the inclusion of "redundant" receptors, likely to show similar responses with respect to all of the compounds, may bias the calculated activity dissimilarity scores. On the other hand, keeping them in the test panel may prove an interesting asset for understanding selectivity issues and in vivo properties in a real drug discovery process. It is nevertheless possible to compensate for these correlations when the

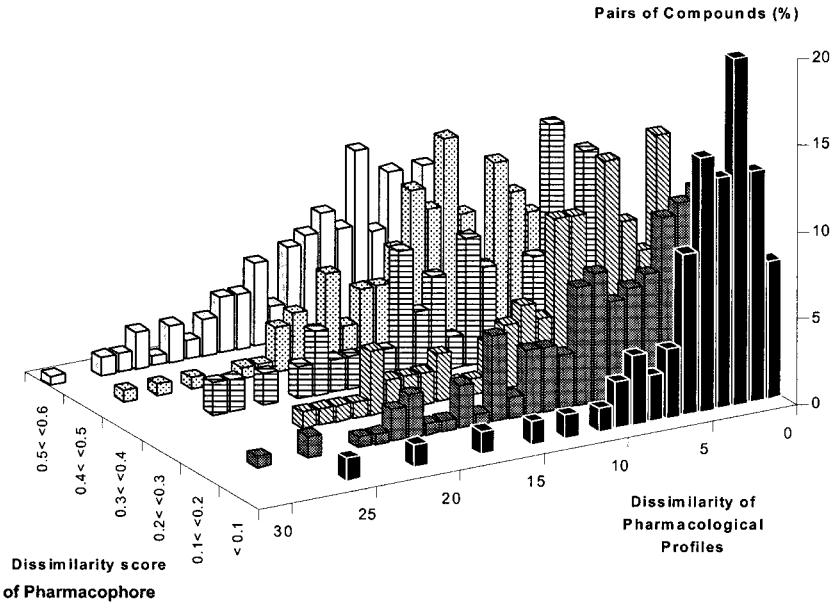

Figure 2. Dissimilarity of pharmacological profiles vs dissimilarity of pharmacophore for each pair of compounds among **1**, **2**, **3**−**37**, and **39**−**48.** Calculated from percentages of inhibition at 10 μM. Dissimilarity of pharmacophore is the dissimilarity score obtained from FBPAs.

activity dissimilarity scores are estimated, by introducing weighing factors for all the receptors, such as to reduce the relative contributions of the members of receptor families known to have similar responses over the structural space. However, to obtain a relevant estimate of the degree of correlation of the responses of two receptors, these should be confronted by a significant sample of the entire structural space of all the "druglike" compounds. The compounds reported in this work cover mainly the subspace that is compatible with an opiate activity and may therefore not be representative of the entire structural space. This is generally the case in medicinal chemistry. Experiments with a significant sample of drugs and druglike molecules showed that accounting for target intercorrelations may somehow modify the fractions of compounds showing a given NR_{diff} at given dissimilarity scores, without nevertheless altering the overall conclusions of the studies.[16]

Pharmacophore dissimilarity scores and the corresponding NR_{diff} values were evaluated for each of the pairwise combinations of the 47 compounds (**1** and **2** and their analogues). These pairs were sorted into dissimilarity categories. The distribution of the pairs in each category versus the observed NR_{diff} values is given in Figure 2. In the class of highly similar compound pairs (pharmacophore dissimilarity score ≤ 0.1), the occurrence of compound pairs with significant profile differences is consistently low. With increasing pharmacophore dissimilarity, the relative probability of finding a pair of compounds with a similar pharmacological profile significantly decreases. The pairs of compounds found similar by the FBPA metric are more likely to have similar pharmacological behavior than any random pair of dissimilar molecules. Interestingly, compounds **10** and **15**, differing only by a methyl group, nevertheless have quite different pharmacological profiles (they display significant differences with respect to 13 targets of the profile), whereas their extremely low pharmacophore dissimilarity score cannot be actually dismissed as an artifact of the similarity metric.

Conclusion

The main purpose of this work was to explore the relationships between pharmacological profiles (a generalized descriptor of biological activity against a battery of relevant targets, defining an "activity space") and chemical structures as typically encountered in the course of primary hit optimization.

In the work presented here, the proposed strategy for optimization relies on one hand on two complementary methods for analogue generation and on the other hand on the compound selection based not only on their affinity for the target, but also on their pharmacological profile.

Chemical structures were situated in a "structural space" defined on the basis of pharmacophore pattern descriptors. This structural space shows a satisfactory "neighborhood behavior" of statistical nature with respect to the "activity space" defined by the pharmacological profile. Indeed, any pair of near neighbors in structure space (similar molecules) are highly likely to also be near neighbors in activity space, e.g., to have similar pharmacological properties. Therefore, in general, no change in the overall specificity should be expected when using an analogue generation based on a quantitative estimation of compound structural similarity in the space of pharmacophoric properties. It appears however to be a strategy of choice to bring into the experiment molecules built on radically different scaffolds and therefore to create new synthesis opportunities for voluntary changes of the pharmacophoric properties. Moreover, this approach allows nonobvious "jumps" to be made in the chemical space and escape from rules dependent, at least partly, on atom connectivity, such as chemical and metabolic stability and even patent claims.

The exploratory approach, open-ended, exploits the diversity of molecular templates provided by the first method and may introduce dramatic changes in the pharmacophoric patterns of the molecules with, as

shown here, radical effects on both their target activity and their pharmacological profile. It is therefore the strategy of choice to pursue the optimization of nonspecific and low activity compounds. In our case, it mainly consisted of a random walk in structural space. However, when structural information on the binding site is available, different modeling tools, not relying on the concept of similarity, should be used to suggest the optimal "moves" to follow to improve potency and selectivity.

To put this into another perspective, our results can be related to the general concept of privileged structures introduced previously by Evans et al.[17] Indeed, as already shown for biphenyl and benzodiazepine frameworks, 1-phenyltriaza-1,3,8-spiro[4.5]decanones, benzimidazolones, and *gem*-diphenylalkanes appear in our work to be able to provide ligands for diverse receptors, especially when coupled to a basic site. Moreover, our demonstration that structural neighbors of promiscuous compounds are more likely to be promiscuous confirms the hypothesis that special structural features underlie the ability of compounds to bind to multiple receptors. With specific examples, we show here, as suggested by Evans and colleagues, that judicious (sometimes minor) modifications of privileged frameworks can provide specific ligands for the opiate receptors. However, the site where modifications are both allowed by the target and beneficial in terms of specificity are not easily predicted. A systematic evaluation of the pharmacological profile of early analogues has proven in our hands to provide valuable directions to tailor the structures and define the best optimization routes.

Experimental Section

Chemistry. General Information. All commercial reagents and solvents were used without further purification. NMR spectra were recorded on either a Bruker DRX-300 or a Bruker DMX-600 spectrometer. Chemical shifts are in parts per million (ppm). The assignments were made using one-dimensional (1D) ^{1}H and ^{13}C spectra and two-dimensional (2D) HMQC spectra. Mass spectra were determined using a Micromass Platform instrument equipped with an APCI interface. SAR-grade compounds were purified by extraction or preparative HPLC using a Shimadzu LC-10 preparative chromatography system equipped with LC-8A pumps, an FRC-10A fraction collector, an SPD-10A detector, and a Vydac C18 5 μm particle size column, dimensions 250 × 25.4 mm. A gradient starting from 100% H_2O and reaching 100% H_2O/80% CH_3CN within 18 min at a flow rate of 50 mL/min was used. Organic layers obtained after extraction of aqueous solutions were dried over $MgSO_4$ and filtered before evaporation in vacuo. Purity was determined by two different HPLC systems. In the first system, analyses were performed using a C18 TSK-GEL Super ODS 3 μm particle size column, dimensions 50 × 4.6 mm. A gradient starting from 100% H_2O/0.05% TFA and reaching 100% H_2O/80% CH_3CN/0.0425% TFA within 5 min at a flow rate of 2.75 mL/min was used (t_R = retention time). Chromatograms were recorded on an LC/MS system using a Micromass Platform instrument coupled with an HP 1100 LC system with a diode array (200−400 nm) detector or using a Micromass ZMD system coupled with a Gilson 307 diode array detector and LC pumps 306. In the second system, analyses were performed on an Adsorbosphere CN 3U from Alltech 3 μm particle size column, dimensions 50 × 4.6 mm, using a Shimadzu instrument equipped with LC-10AS pumps and an SPD-10A dual wavelength detector. A gradient starting from 100% H_2O/0.05% TFA and reaching 100% H_2O/80% CH_3CN/0.0425% TFA within 25 min at a flow rate of 2.75 mL/min was used (t_R' = retention time). Purification yields were not optimized. Melting points were measured on a Büchi B-450 apparatus and are uncorrected. All the reactions on the 5 μmol scale were performed in 96-well polypropylene plates, Beckmann reference 26 7006. When more material was needed (SAR grade compounds), the reactions were performed 30 or 40 times in the same conditions and reaction products pooled before purification.

General Procedure A for Carbamates. A 42 μL (10.3 μmol, 2.1 equiv) sample of a solution (0.247 M, in THF) of *N*,*N*′-carbonyldiimidazole was added at room temperature to 50 μL (5 μmol, 1 equiv) of a solution (0.1 M, in DMF) of alcohol. After the resulting solution was stirred at room temperature for 2 h, 50 μL (5 μmol, 1 equiv) of a solution (0.1 M, in DMF) of amine was added. The reaction mixture was stirred overnight and then evaporated under reduced pressure. The residue was purified by preparative HPLC.

General Procedure B for Amides. A 42 μL (10.3 μmol, 2.1 equiv) sample of a solution (0.247 M, in THF) of *N*,*N*′-carbonyldiimidazole was added at room temperature to 9 μL (5 μmol, 1 equiv) of a solution (0.56 M, in DMF) of acid. After the resulting solution was stirred at room temperature for 2 h, 50 μL (5 μmol, 1 equiv) of a solution (0.1 M, in DMF) of amine was added. The reaction mixture was stirred for 2 h and then evaporated under reduced pressure. The residue was purified by preparative HPLC.

General Procedure C for Ureas. A 42 μL (10.3 μmol, 2.1 equiv) sample of a solution (0.247 M, in THF) of *N*,*N*′-carbonyldiimidazole was added at room temperature to 50 μL (5 μmol, 1 equiv) of a solution (0.1 M, in DMF) of the first amine. After the resulting solution was stirred at room temperature for several minutes, 50 μL (5 μmol, 1 equiv) of a solution (0.1 M, in DMF) of the second amine was added. The reaction mixture was stirred overnight and then evaporated under reduced pressure. The residue was purified by preparative HPLC.

4-[4,4-Bis(4-fluorophenyl)butyl]piperazine-1-carboxylic Acid 2-(4-Cyanophenyl)ethyl Ester (2) (Procedure A). HPLC: t_R = 2.56 min and t_R' = 14.4 min. ^{1}H NMR (DMSO-d_6, 300 MHz): δ 1.37 (m, 2H), 2.06 (dt, J = 7.8 Hz, J' = 7.3 Hz, 2H), 2.28 (br s, 4H), 2.36 (t, J = 7.1 Hz, 2H), 3.05 (t, J = 6.4 Hz, 2H), 3.33 (br s, 4H), 4.05 (t, J = 7.9 Hz, 1H), 4.29 (t, J = 6.5 Hz, 2H), 7.18 (t, $J_{H-H} = J_{H-F}$ = 8.8 Hz, 4H), 7.40 (dd, J_{H-H} = 8.7 Hz, J_{H-F} = 5.6 Hz, 4H), 7.54 (d, J = 8.2 Hz, 2H), 7.85 (t, J = 8.2 Hz, 2H). ^{13}C NMR (DMSO-d_6, 300 MHz): δ 25.2, 33.3, 35.4, 43.9, 49.3, 52.9, 57.9, 65.3, 109.9, 115.8 (J_{C-F} = 83 Hz), 119.6 (*C*N), 129.9 (J_{C-F} = 32 Hz), 130.7, 132.8, 141.9, 145.2, 154.9 (N*C*OO), 162.9. MS (APCI+): m/z 505 $[M + H]^+$.

{1-[4,4-Bis(4-fluorophenyl)butyl]piperidin-4-yl}-amine Dihydrochloride (38). A mixture of 1,1-(4-chlorobutylidene)bis(4-fluorobenzene) (3 g, 10.7 mmol) and 4-[*N*-(*tert*-butyloxycarbonyl)amino]piperidine (1.95 g, 9.7 mmol) in CH_3CN (17.7 mL) and DIPEA (3.72 mL) was refluxed for 4 days. The reaction mixture was then evaporated under reduced pressure to give a brown oil. Flash chromatography on silica gel with CH_2Cl_2/MeOH (95:5) as the solvent system afforded 2.69 g of a yellow oil. A solution of the protected amine intermediate was refluxed for 2 h in HCl (3 N, in EtOH) (50 mL). The reaction mixture was evaporated under reduced pressure to give a beige solid. Trituration with Et_2O/pentane (50:50) (2 × 20 mL) afforded 2.25 g of the beige dihydrochloride salt (55%). HPLC: t_R = 1.97 min. ^{1}H NMR (DMSO-d_6, 300 MHz): δ 1.53−1.55 (m, 2H), 1.84−2.11 (m, 6H), 2.83−3.02 (m, 4H), 3.18−3.26 (m, 1H), 3.32−3.40 (m, 2H), 3.97 (t, J = 7.53 Hz, 1H), 7.09 (t, $J_{H-F} = J_{H-H}$ = 8.8 Hz, 4H), 7.32 (dd, J_{H-H} = 8.6 Hz, J_{H-F} = 5.5, 4H), 8.40 (br s, 3H, H_3N^+), 10.52 (s, 1H, NH^+). MS (APCI+): m/z 345.4 $[M + H]^+$.

4-[4,4-Bis(4-fluorophenyl)butyl]piperazine-1-Carboxylic Acid 2-(4-fluorophenyl)ethyl Ester (39) (Procedure A). HPLC: t_R = 2.63 min and t_R' = 14.54 min. ^{1}H NMR (DMSO-d_6, 600 MHz): δ 1.37 (m, 2H), 2.06 (dt, J = 7.8 Hz, J' = 7.3 Hz, 2H), 2.28 (br s, 4H), 2.36 (t, J = 7.1 Hz, 2H), 3.05 (t, J = 6.4 Hz, 2H), 3.33 (br s, 4H), 4.05 (t, J = 7.9 Hz, 1H), 4.29 (t, J = 6.5 Hz, 2H), 7.05 (t, $J_{H-H} = J_{H-F}$ = 8.9 Hz, 4H), 7.06 (t, $J_{H-H} = J_{H-F}$ = 8.9 Hz, 2H), 7.22 (dd, J_{H-H} = 8.6 Hz, J_{H-F} =

5.6 Hz, 2H), 7.27 (dd, J_{H-H} = 8.6 Hz, J_{H-F} = 5.6 Hz, 4H). ^{13}C NMR (DMSO-d_6, 300 MHz): δ 27.3, 35.1, 36.1, 45.1, 50.3, 54.5, 58.9, 66.8, 109.9, 116.6, 116.9, 131.0, 132.6. MS (APCI+): *m/z* 498 $[M + H]^+$.

1-{4-[4,4-Bis(4-fluorophenyl)butyl]piperazin-1-yl}-3-(4-fluorophenyl)propan-1-one (40) (Procedure B). HPLC: t_R = 2.47 min and t_R' = 14.14 min. ^{1}H NMR (DMSO-d_6, 600 MHz): δ 1.19−1.29 (m, 2H), 1.93 (dt, J = 7.8 Hz, J' = 7.3 Hz, 2H), 2.14 (br s, 4H), 2.21 (t, J = 7.1 Hz, 2H), 2.52 (t, J = 7.8 Hz, 2H), 2.73 (t, J = 7.3 Hz, 2H), 3.29−3.31 (m, 4H), 3.92 (t, J = 7.9 Hz, 1H), 7.03 (t, J_{H-H} = J_{H-F} = 8.9 Hz, 2H), 7.05 (t, J_{H-H} = J_{H-F} = 8.9 Hz, 4H), 7.21 (dd, J = 8.5 Hz, J_{H-F} = 5.6 Hz, 2H), 7.27 (dd, J = 8.5 Hz, J_{H-F} = 5.6 Hz, 4H). ^{13}C NMR (DMSO-d_6, 300 MHz): δ 26.2, 31.4, 34.2, 35.4, 42.5, 46.4, 50.2, 54.2, 58.7, 116.4, 116.7, 132.4, 132.0. MS (APCI+): *m/z* 481 $[M + H]^+$.

4-(3-Phenylpropyl)piperazine-1-carboxylic Acid 2-(4-Cyanophenyl)ethyl Ester (41) (Procedure A). HPLC: t_R = 2.11 min. ^{1}H NMR (DMSO-d_6, 600 MHz): δ 1.66 (m, 2H), 2.19−2.24 (m, 6H), 2.53 (t, J = 7.5 Hz, 2H), 2.93 (t, J = 6.5 Hz, 2H), 3.24−3.26 (m, 4H), 4.18 (t, J = 6.5 Hz, 1H), 7.10−7.16 (m, 3H), 7.20−7.25 (m, 2H), 7.41 (d, J = 8.4 Hz, 2H), 7.73 (d, J = 8.4 Hz, 2H). ^{13}C NMR (DMSO-d_6, 300 MHz): δ 29.5, 34.4, 36.4, 44.8, 54.1, 57.9, 66.2, 126.8, 129.8, 131.7, 133.7. MS (APCI+): *m/z* 378 $[M + H]^+$.

4-(3-Phenylallyl)piperazine-1-carboxylic Acid 2-(4-Cyanophenyl)ethyl Ester (42) (Procedure A). HPLC: t_R = 2.08 min. ^{1}H NMR (DMSO-d_6, 600 MHz): δ 2.31 (br s, 4H), 2.98 (t, J = 6.4 Hz, 2H), 3.09 (dd, J = 6.7 Hz, J' = 1 Hz, 2H), 4.22 (t, J = 6.5 Hz, 2H), 6.23 (dt, J = 6.6 Hz, J = 15.9 Hz, 1H), 6.53 23 (d, J = 15.9 Hz, 1H), 7.23 (t, J = 7.3 Hz, 1H), 7.32 (t, J = 7.8 Hz, 2H), 7.44 (d, J = 7.1 Hz, 2H), 7.45 (t, J = 8.3 Hz, 2H), 7.76 (d, J = 8.3 Hz, 2H). MS (APCI+): *m/z* 376 $[M + H]^+$.

4-(3-Phenylpropyl)piperazine-1-carboxylic Acid 2-(4-Ethoxyphenyl)ethyl Ester (43) (Procedure A). HPLC: t_R = 2.47 min and t_R' = 12.36 min. ^{1}H NMR (DMSO-d_6, 600 MHz): δ 1.25 (t, J = 6.9 Hz, 2H), 1.66 (m, 2H), 2.19−2.24 (m, 6H), 2.53 (t, J = 7.5 Hz, 2H), 2.74 (t, J = 6.8 Hz, 2H), 3.24−3.26 (m, 4H), 3.93 (q, J = 6.9 Hz, 2H), 4.08 (t, J = 6.8 Hz, 1H), 6.78 (d, J = 8.7 Hz, 2H), 7.08 (d, J = 8.7 Hz, 2H), 7.10−7.16 (m, 3H), 7.22 (t, J = 7.3 Hz, 2H). ^{13}C NMR (DMSO-d_6, 300 MHz): δ 16.3, 29.5, 34.4, 35.4, 44.8, 54.1, 57.9, 64.4, 66.9, 115.8, 127.2, 129.8, 131.3. MS (APCI+): *m/z* 397 $[M + H]^+$.

4-[4,4-Bis(4-fluorophenyl)butyl]piperazine-1-carboxylic Acid [2-(4-Ethoxyphenyl)ethyl]amide (44) (Procedure C). HPLC: t_R = 2.80 min and t_R' = 14.37 min. ^{1}H NMR (DMSO-d_6, 600 MHz): δ 1.25 (m, 5H), 1.94 (dt, J = 7.7 Hz, J' = 7.3 Hz, 2H), 2.14 (br s, 4H), 2.22 (t, J = 7.4 Hz, 2H), 2.56 (t, J = 8.2 Hz, 2H), 3.07−3.12 (m, 2H), 3.16 (m, 4H), 3.91 (t, J = 7.0 Hz, 1H), 3.93 (t, J = 7.0 Hz, 2H), 6.46 (t, J = 5.3 Hz, 1H, N*H*CO), 6.77 (d, J = 8.6 Hz, 2H), 7.03 (d, J = 8.6 Hz, 2H), 7.05 (t, J_{H-H} = J_{H-F} = 8.9 Hz, 4H), 7.28 (dd, J_{H-H} = 8.9 Hz, J_{H-F} = 5.6 Hz, 4H). ^{13}C NMR (DMSO-d_6, 300 MHz): δ 16.2, 26.2, 34.1, 36.6, 43.4, 45, 50.3, 54.1, 58.9, 64.4, 115.6, 116.6, 130.7, 130.9. MS (APCI+): *m/z* 522 $[M + H]^+$.

1-{4-[4,4-Bis(4-fluorophenyl)butyl]piperazin-1-yl}-4-phenylbutan-1-one (45) (Procedure B). HPLC: t_R = 2.61 min and t_R' = 14.46 min. ^{1}H NMR (DMSO-d_6, 600 MHz): δ 1.19−1.29 (m, 2H), 1.66−1.76 (m, 2H), 1.94 (dt, J = 7.8 Hz, J' = 7.2 Hz, 2H), 2.15−2.18 (m, 6H), 2.23 (t, J = 7.3 Hz, 2H), 2.52 (t, J = 7.8 Hz, 2H), 3.28−3.35 (m, 4H), 3.93 (t, J = 7.9 Hz, 1H), 7.05 (t, J_{H-H} = J_{H-F} = 8.9 Hz, 5H), 7.13 (d, J = 7.1 Hz, 2H), 7.22 (t, J = 6.6 Hz, 2H), 7.27 (dd, J_{H-H} = 8.5 Hz, J_{H-F} = 5.6 Hz, 4H). ^{13}C NMR (DMSO-d_6, 300 MHz): δ 26.0, 27.9, 32.7, 33.7, 36.0, 42.3, 46.0, 50.2, 53.9, 59.4, 116.7, 129.7, 129.9, 130.9. MS (APCI+): *m/z* 477 $[M + H]^+$.

{4-[4,4-Bis(4-fluorophenyl)butyl]piperidin-1-yl}carbamic Acid 2-(4-Cyanophenyl)ethyl Ester (46). The title compound was prepared from **38** according to procedure A. HPLC: t_R = 2.56 min and t_R' = 14.3 min. ^{1}H NMR (DMSO-d_6, 600 MHz): δ 1.19−1.33 (m, 4H), 1.58 (d, J = 10.8 Hz, 2H), 1.75 (t, 2H), 1.91 (dt, J = 7.3 Hz, J' = 7.6 Hz, 2H), 2.17 (t, J = 7.0 Hz, 2H), 2.62 (d, 2H), 2.89 (t, J = 6.7 Hz, 2H), 2.94−3.21 (m, 1H), 3.92 (t, J = 7.9 Hz, 1H), 4.11 (t, J = 6.6 Hz, 2H), 7.04 (t, J_{H-H} = J_{H-F} = 8.9 Hz, 4H), 7.26 (dd, J_{H-H} = 8.8 Hz, J_{H-F} = 5.6 Hz, 4H), 7.41 (d, J = 8.3 Hz, 2H), 7.71 (d, J = 8.3 Hz, 2H). ^{13}C NMR (DMSO-d_6, 300 MHz): δ 25.2, 35.4, 39.4, 43.9, 49.3, 52.9, 57.9, 65.3, 109.9, 115.8 (J_{C-F} = 83 Hz), 119.6 (*C*N), 129.9 (J_{C-F} = 32 Hz), 130.7, 132.8, 141.9, 145.2, 154.9 (NCOO), 162.9. MS (APCI+): *m/z* 519 $[M + H]^+$.

1-{4-[3-(4-Chlorophenoxy)benzyl]piperazin-1-yl}-3-(4-methoxyphenylsulfanyl)propan-1-one (47) (Procedure B). HPLC: t_R = 2.52 min and t_R' = 14.4 min. ^{1}H NMR (DMSO-d_6, 600 MHz): δ 2.35−2.41 (m, 4H), 2.63 (t, J = 7.2 Hz, 2H), 3.10 (t, J = 7.2 Hz, 2H), 3.42−3.45 (m, 2H), 3.48−3.52 (m, 2H), 3.56 (s, 2H), 3.82 (s, 3H), 6.99 (d, J = 8.8 Hz, 2H), 7.0 (dd, J = 7.7 Hz, J' = 1.0 Hz, 1H), 7.06 (m, 1H), 7.11 (d, J = 9.0 Hz, 2H), 7.19 (dd, J = 7.7 Hz, J' = 1.0 Hz, 1H), 7.41 (d, J = 8.9 Hz, 2H), 7.44 (dt, J = 7.8 Hz, J' = 0.5 Hz, 1H), 7.52 (d, 2H). ^{13}C NMR (DMSO-d_6, 300 MHz): δ 30.99, 33.1, 41.8, 45.4, 52.8, 53.3, 55.9, 61.9, 115.5, 118.1, 119.6, 120.9, 124.9, 126.6, 127.8, 130.6, 132.9, 141.1, 156.4, 156.9, 159.0, 169.4 (NCO). MS (APCI+): *m/z* 498 $[M + H]^+$.

1-{4-[3-(Benzyloxy)-4-methoxybenzyl]piperazin-1-yl}-3-(3-methylindol-1-yl)propan-1-one (48) (Procedure B). HPLC: t_R = 2.53 min and t_R' = 13.85 min. ^{1}H NMR (DMSO-d_6, 600 MHz): δ 2.10−2.15 (m, 2H), 2.20−2.25 (m, 2H), 2.31 (s, 3H), 2.84 (t, J = 6.8 Hz, 2H), 3.28−3.45 (m, 2H), 3.41 (s, 2H), 3.48−3.52 (m, 2H), 3.82 (s, 3H), 4.41 (t, J = 6.8 Hz, 2H), 5.13 (s, 2H), 6.86 (dd, J = 8.1 Hz, 1H), 6.98 (d, J = 5.7 Hz, 2H), 7.00 (s, 1H), 7.08 (dt, J = 7.9 Hz, J' = 1.0 Hz, 1H), 7.19 (dt, J = 1.2 Hz, J' = 8.3 Hz, 1H), 7.20 (d, J = 1.0 Hz, 1H), 7.33−7.57 (m, 5H). ^{13}C NMR (DMSO-d_6, 300 MHz): δ 10.14, 33.64, 41.8, 45.4, 52.6, 53.0, 56.2, 62.0, 70.5, 110.2, 112.5, 115.2, 118.9, 119.1, 121.7, 125.4, 127.7, 128.4, 129.0, 135.5, 137.8, 140.9, 148.0, 149.0, 169.4 (NCO). MS (APCI+): *m/z* 499 $[M + H]^+$.

Molecular Modeling. All computations were performed on desktop Silicon Graphics workstations using a proprietary software note integrated into Cerius^2 environment thanks to the software developer kit (SDK) from Molecular Simulations Inc. (San Diego, CA).

Receptor Binding Assays. The affinities for the different receptors were determined using conventional in vitro receptor binding methodology. All incubations of the radioligand with membranes, and the studied compounds or the nonspecific product, were terminated by adding cold buffer followed by rapid filtration using a cell harvester from Packard. Bound radioactivity was counted using a Topcount from Packard, thanks to a scintillation liquid (Formula 989 or Microscint from Packard). Reference compounds were run in duplicate, using at least eight concentrations. All IC_{50} calculations were done using nonlinear regression.

Compounds were first tested at 10 μM in duplicate. Compounds with a percentage of inhibition above 80% on a target were selected for IC_{50} calculation on that target. All IC_{50} experiments were done with eight concentrations, and calculations were done using nonlinear regression.

Experimental conditions for the 75 binding tests are given in the Supporting Information.

Acknowledgment. We are grateful to P. George for his skillful help and G. Montagne for the NMR spectra.

Supporting Information Available: Experimental conditions and references for all the binding tests of the high-throughput profile, NMR spectra, mass spectra, and HPLC chromatograms for all the compounds described in the Experimental Section. This material is available free of charge via the Internet at http://pubs.acs.org.

References

(1) Kordel, J. Relieving bottlenecks: establishing criteria for lead generation and lead optimization early in the discovery pipeline to create a seamless flow of information. *Optimizing Candidate Selection, Vision in Business*, Basel CH, Switzerland, Dec 1−2, 1998.

(2) See the previous paper in this issue: Poulain, R.; Horvath, D.; Eckhoff, C.; Chapelain, B.; Bodinier, M.-C.; Déprez, B. From Hit to Lead. Combining Two Complementary Methods for Focused Library Design. Application to μ opiate ligands. *J. Med. Chem.* **2001**, *44*, 3378−3390.

(3) Bolognesi, M. L.; Ojala, W. H.; Gleason, W. B.; Griffin, J. F.; Farouz-Grant, F.; Larson, D. L.; Takemori, A. E.; Portoghese, P. S. Opioid Antagonist Activity of Naltrexone-Derived Bivalent Ligands: Importance of a Properly Oriented Molecular Scaffold To Guide ⟨⟨Address⟩⟩ Recognition at κ Opioid Receptors. *J. Med. Chem.* **1996**, *39*, 1816−1822. Zimmerman, D. M.; Leander, J. D. Selective Opioid Receptor Agonists and Antagonists: Research Tools and Potential Therapeutic Agents. *J. Med. Chem.* **1990**, *33*, 895−902. Portoghese, P. S. The Role of Concepts in Structure−Activity Relationship Studies of Opioid Ligands. *J. Med. Chem.* **1992**, *35*, 1927−1937. Fournie-Zaluski, M.-C.; Gacel, G.; Maigret, B.; Premilat, S.; Roques, B. P. Structural Requirements for Specific Recognition of Mu or Delta Opiate Receptors. *Mol. Pharmacol.* **1981**, *20*, 484−491.

(4) Beck-Sickinger, A. G. Structural characterization and binding sites of G-protein-coupled receptors. *DDT* **1996**, *1*, 502−513.

(5) In this paper, the word pharmacophore is used in a sense differing from the definition given by IUPAC (Wermuth, C.-G.; Ganellin, C. R.; Lindberg, P.; Mitscher, L. A. Glossary of terms used in Medicinal Chemistry (IUPAC recommendations 1997). *Annu. Rep. Med. Chem.* **1998**, *33*, 385−395). Pharmacophore refers here to the ensemble of all steric and electronic features of a given molecule, which could potentially ensure interactions with a biological target structure.

(6) See ref 2 for theoretical details of method B, definition of FBPAs (fuzzy bipolar autocorrelograms) and calculation of the dissimilarity score between two compounds using the FBPA metric.

(7) Horvath, D. High Throughput Conformational Sampling and Fuzzy Similarity Metrics: A Novel Approach to Similarity Searching and Focused Combinatorial Library Design and its Role in the Drug Discovery Laboratory. In *Combinatorial Library Design and Evaluation: Principles, Software Tools and Applications*; Ghose, A. K., Vishwadhan, V. N., Eds.; Marcel Dekker: New York, in press.

(8) Horvath, D. ComPharm−Automated Comparative Analysis of Pharmacophoric Patterns and Derived QSAR Approaches, Novel Tools in High-Throughput Drug Discovery. A Proof of Concept Study Applied to Farsenyl Transferase Inhibitor Design. In *QSPR/QSAR Studies by Molecular Descriptors*; Diudea, M., Ed.; Nova Science Publishers: New York, 2001; pp 395−439.

(9) See ref 2 for experimental details of the synthesis of all the mentioned analogues of **1**.

(10) Unpublished results.

(11) Spencer, R. W. High-Throughput Screening of Historic Collections: Observations on File Size, Biological Targets and File Diversity. *Biotechnol. Bioeng. (Comb. Chem.)* 1998, *61* (1), 61−67.

(12) Anzali, S.; Mederski, W. W. K. R.; Osswald, M.; Dorsch, D. 1-Endothelin antagonists: Search for surrogates of methylenedioxyphenyl by means of a kohonen neural network. *Bioorg. Med. Chem. Lett.* **1998**, *8*, 11−16. Mederski, W. W. K. R.; Osswald, M.; Dorsch, D.; Anzali, S.; Christadler, M.; Schmitges, C.-J.; Wilm, C. 2-Endothelin antagonists: Evaluation of 2,1,3-benzothiadiazole as a methylendioxyphenyl bioisoster. *Bioorg. Med. Chem. Lett.* **1998**, *8*, 17−22. Mederski, W. W. K. R.; Dorsch, D.; Osswald, M.; Anzali, S.; Christadler, M.; Schmitges, C.-J.; Schelling, P.; Wilm, C.; Fluck, M. 3-Endothelin antagonists: Discovery of EMD 122946, A highly potent and orally active ET_A selective antagonist. *Bioorg. Med. Chem. Lett.* **1998**, *8*, 1771−1776.

(13) It was recently shown that 8-acenaphthen-1-yl-1-phenyl-1,3,8-triazaspiro[4,5]decan-4-one displays activities on ORL-1: Wichmann, J.; Adam, G.; Röver, S.; Cesura, A. M.; Dautzenberg, F. M.; Jenck, F. 8-acenaphthen-1-yl-1-phenyl-1,3,8-triaza-spiro[4.5]-decan-4-one derivatives as orphanin FQ receptor agonists. *Bioorg. Med. Chem. Lett.* **1999**, *9*, 2343−2348. Röver, S.; Wichmann, J.; Jenck, F.; Adam, G.; Cesura, A. M. ORL-1 Receptor Ligands: Structure−Activity Relationships of 8-cycloalkyl-1-phenyl-1,3,8-triaza-spiro[4.5]decan-4-ones. *Bioorg. Med. Chem. Lett.* **2000**, *10*, 831−834. Röver, S.; Adam, G.; Cesura, A. M.; Galley, G.; Jenck, F.; Monsma, F. J.; Wichmann, J.; Dautzenberg, F. M. High Affinity, Non-peptide Agonists for the ORL-1 (Orphanin FQ/Nociceptin) Receptor. *J. Med. Chem.* **2000**, *43*, 1329−1338.

(14) This can be related to the results obtained previously by Leysen et al. showing that, in a series derived from pimozide, a shortening of the chain between the benzhydryl and the basic nitrogen leads to a shift from neuroleptic to opiate activity: Leysen, J.; Tolenaere, J. P.; Koch, M.; Laduron, P. Differentiation of opiate and neuroleptic receptor binding in rat brain. *Eur. J. Pharmacol.* **1977**, *43*, 253−257.

(15) Roufos, I.; Hays, S.; Schwarz, R. D. A Structure−Activity Relationship Study of Novel Phenylacetamides Which Are Sodium Channel Blockers. *J. Med. Chem.* **1996**, *39*, 1514−1520.

(16) Unpublished results.

(17) (a) Evans, B. E.; Rittle, K. E.; Bock, M. G.; DiPardo, R. M.; Freidinger, R. M.; Whitter, W. L.; Lundell, G. F.; Veber, D. F.; Anderson, P. S.; Chang, R. S., et al. Methods for drug discovery: Development of potent, selective, orally effective cholecystokinin antagonists. *J. Med. Chem.* **1988**, *31*, 2235−2246. (b) For a review on privileged structures see: Patchett, A.; Nargund, R. Privileged Structures-An update. *Annu. Rep. Med. Chem.* **2000**, *35*, 289−298.

JM010878G